Nonlinear beam tapering and two-dimensional ring solitons

V. K. Mezentsev,[1,2] E. Podivilov [©],[2] I. A. Vaseva,[1,3] M. P. Fedoruk [©],[1] A. M. Rubenchik,[4] and S. K. Turitsyn[5]

[1]*Novosibirsk State University, Novosibirsk 630090, Russia*

[2]*Institute of Automation and Electromerty, Siberian Branch RAN, Novosibirsk 630090, Russia*

[3]*Institute of Computational Technologies, Siberian Branch RAS, Novosibirsk 630090, Russia*

[4]*Lawrence Livermore National Laboratory, Livermore, California 94550, USA*

[5]*Aston Institute of Photonic Technologies, Aston University, Birmingham B4 7ET, United Kingdom*

We examine a possibility to exploit the nonlinear lens effect—the initial stage of self-focusing to localize initially broad field distribution into the small central area where wave collapse is arrested—the nonlinear beam tapering. We describe two-dimensional localized solitary waves (ring solitons) in a physical system that presents a linear medium in the central core, surrounded by the cladding with the focusing Kerr nonlinearity. The standard variational analysis demonstrates that such solitons correspond to the minimum of the Hamiltonian.

I. INTRODUCTION

Spatial or temporal localization of energy is a common feature of many physical systems. Confinement of the field can arise from the extrinsic disorder, as in the Anderson localization, or from the nonlinear phenomena as in the soliton theory. In the soliton systems localization is often provided by the balance between dispersion and diffraction (leading to temporal and spatial spreading of linear waves) and the nonlinear effects inducing to self-focusing type wave dynamics. We would like to point our from the start, that the problem we consider is different both from: (i) The light trapping in the center of the hollow core fibers that is implemented by the linear wave guiding, and (ii) the existing mechanism of the field localization in the hollow core fiber that again has nothing to do with the nonlinear self-focusing considered here.

The process of the energy transfer from large spatial scales to small ones can either keep coherence of the field during squeezing (as, e.g., in a tailored taper) or be of a turbulent-like nature, involving interactions of many uncorrelated degrees of freedom [1]. Mechanisms of the transition from the extended fields to the states with the spatially localized energy are important both in the fundamental science (e.g., pattern formation, generation of the coherent structures, localization by disorder, and so on) and in various practical applications (e.g., capturing light, sound, or other waves in a waveguide).

There are two typical problems related to the energy localization: How confined waves are stabilized and how initially broad—extended field distributions can be aggregated into a small area. In this paper we examine both problems considering specific modification of the classical nonlinear model—two-dimensional nonlinear Schrödinger equation (NLSE) with an insertion of the linear medium near the center.

It is well known that in the two-dimensional NLSE the field (e.g., light beam) with power above critical experiences self-focusing (wave collapse) (see, e.g., Refs. [2–5] and references therein). Wave collapse can be stopped by various physical effects neglected in the main order master model (for a comprehensive review of the collapse arrest see Refs. [2,3,6–10] and numerous references therein).

Consider the medium with the Kerr nonlinearity with the nonlinear coefficient n_2 to be higher in the outer area compared to the central hole and core. We do not specify the geometry of the outer region, considering it here to be much larger than the central area that we for simplicity assume to be a circle. However, the proposed concept can be easily adjusted to the design of the particular nonlinear system. For instance, in the optical applications context, this can be the hollow core embedded in the medium with the higher nonlinearity material.

We consider a possibility of exploiting initial self-focusing mechanism to transfer the energy from the broad spatial area to the small region with the reduced nonlinearity (e.g., air hole, or hollow core, depending on the specific implementation) where collapse is arrested. Nonlinearity in the area outside the hole acts as an optical lens for the power localization. This system acts as a funnel, or an effective nonlinear taper, transferring energy from the broad area harvesting incoming power to the small central core.

II. MATHEMATICAL MODEL

Without loss of generality we will use optical terminology when discussing the master model, although its applications are much broader and can be found in a large number of physical systems (see, e.g., Ref. [11] and references therein). Evolution of an envelope of a quasimonochromatic optical beam with a single polarization is governed by the nonlinear partial differential equation—the NLSE (see, e.g., Refs. [2,11] and references therein), that accounts for the major propagation effects, such as diffraction (for the sake of clarity we

assume that linear characteristics are the same in the core and the surrounding area) and Kerr nonlinearity,

$$i\frac{\partial \Psi}{\partial Z} + \frac{1}{2n_0 k_0}\Delta'_{\perp}\Psi + k_0 n_2(r)|\Psi|^2\Psi + \delta n_0(r)\Psi = 0. \quad (1)$$

$\Psi(x', y', Z)$ is the envelope of the electric field, and the beam is propagating along the Z axis, $\Delta'_{\perp}$ is a two-dimensional transverse Laplacian operator, $\vec{r}'_{\perp} = (x', y')$'s are the transverse coordinates, $r'^2_{\perp} = x'^2 + y'^2$, $k_0 = 2\pi/\lambda_0$ is the wave number in the medium, λ_0 is the vacuum wavelength, n_0 is the linear index of refraction, and n_2 is the nonlinear Kerr index. The index of refraction is $n = n_0 + \delta n_0(r'_{\perp}) + n_2(r'_{\perp})I$. It is assumed here that the temporal duration of the field is long enough to neglect time-dependent effects (dispersion). It is convenient to rewrite the NLSE in the dimensionless Hamiltonian form by the straightforward scaling transformation $|A(x, y, z)|^2 = [k_0^2 n_0 \max(n_2)]|\Psi(x', y', Z|^2)$, $z = n_0 k_0 Z$, $r = n_0 k_0 r'_{\perp}$,

$$i\frac{\partial A}{\partial z} = -\frac{1}{2}\vec{\nabla}^2_{\perp}A - V(r)|A|^2 A - U(r)A = \frac{\delta H}{\delta A^*}, \quad (2)$$

here Hamiltonian H is defined as

$$2H = \int |\vec{\nabla}_{\perp}A|^2 d\vec{r} - \int V|A|^4 d\vec{r} - 2\int U|A|^2 d\vec{r}.$$

We present below all the results in the general normalized form. Apparently, Eq. (2) conserves the total power $N = \int |A|^2 d\vec{r}$ along with the Hamiltonian H. It is well known that the conventional NLSE—Eq. (2) (U and V are constants) describes the catastrophic collapse of the average radius of the beam $R = \int r^2|A|^2 d\vec{r}$ [12], provided that $H < 0$. Condition $H < 0$ is satisfied when a beam power exceeds the critical value N of the self-focusing $N_{cr} \approx 5.85$. The impact of the linear potential on the self-focusing has been studied in Ref. [13]. The main conclusion was that the wave collapse can be delayed (in z) by the external linear potential. To stress that the linear wave guiding is not required in the central part, in what follows we drop a linear potential $U = 0$ and consider the situation when the central area differs from the outside medium only by the nonlinear properties (no nonlinearity, or in the more practical terms, much higher nonlinear threshold). This point illustrates the difference between the problem we consider here and light localization in the hollow core fiber where nonlinear effects are not important at all for both collecting light in the small core area and keeping energy in this core. In the hollow core fiber light localization is defined by the (linear) waveguide that is opposite to nonlinear-based localized considered here.

III. CONTRACTION DYNAMICS

It is evident that if the central area has no nonlinearity ($V = 0$), the wave collapse is arrested. In the case of a nonuniform distribution of nonlinearity using the chain of inequalities following Ref. [14] we can prove for $V(x, y)$ satisfying certain conditions that the integral $R = \int r^2|A|^2 d\vec{r}$ is bounded from below. This also gives an estimate on the possible compression of the average radius of the beam. Let us define $I_d = \int |\nabla A|^2 d\vec{r}$, $I_k = \int |A|^k d\vec{r}$ and use the inequalities [14–16]:
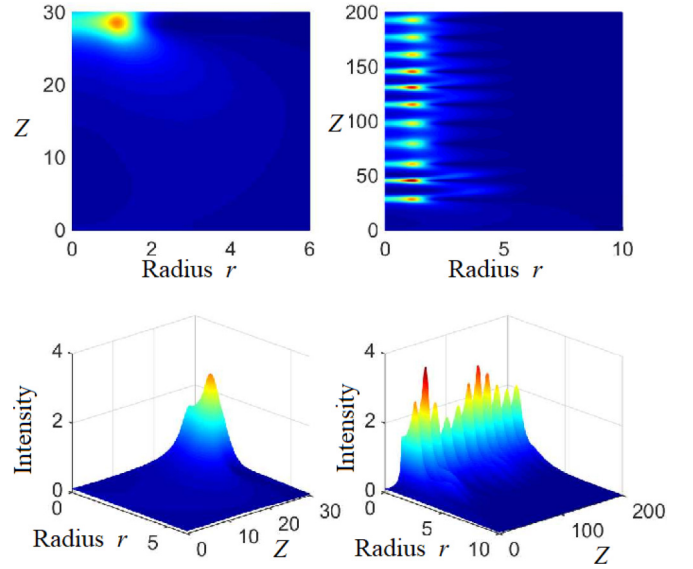

FIG. 1. Evolution of the intensity profile $I(r, z)$ (upper figures—contour plots, bottom—three-dimensional (3D) dynamics) for a Gaussian input signal with $a = 10$, $N = 12\pi$. Left: The initial stage of the compression from $z = 0$ to 30.

(i) $\int V|A|^4 d\vec{r} \leqslant I_6^{1/2}(\int V^2|A|^2 d\vec{r})^{1/2}$,

(ii) $I_6 \leqslant 9 I_4 I_d \leqslant 9 N I_d^2/N_{cr}$.

Assuming that we deal with the function $V(x, y)$ satisfying condition: $\max_{x,y}(V^2/r^2) = B_0 < \infty$, it is straightforward to derive.

$$2H = I_d - \int V|A|^4 d\vec{r} \geqslant I_d\left[1 - \left(\frac{R}{R_l}\right)^{1/2}\right].$$

Here $R_l = N_{cr}/(9B_0 N) > 0$. Straightforward manipulations show that when $H < 0$ (that is the condition of collapse in the standard NLSE) we get a lower bound on R for any z,

$$R \geqslant R_l(1 - 2H/I_d)^2 \geqslant R_l.$$

Figure 1 depicts (contour plots and 3D) evolution of the intensity profile $I(r, z)$ for a Gaussian input beam $A(r, 0) = \sqrt{N/(a^2\pi)}\exp[-r^2/(2a^2)]$ with a radius $a = 10$ and power $N = 12\pi$. Figure 1 shows results of a numerical solution of the NLSE (2) with a central circle area of a radius $R_0 = 1$ where the nonlinear parameter $V = 0$, whereas outside the hole $V = 1$. At the initial stage shown in Fig. 1 (left), the beam is compressed from the initially broad distribution towards the center. After that initial compression a typical dynamics presents a breathing type oscillatory evolution characteristic to the conservative system. The oscillating dynamics features periodic increases and decreases of the intensity with the corresponding compression or broadening of the beamwidth. Note that these oscillations of the beam width occur at the scales much smaller than the initial beam radius.

Figure 2 shows corresponding evolution of the fraction of the total power $N_{trapped}/N$ trapped after initial compression inside the small region around the hole in the region of $r \in [0\ R_{trapped}]$,
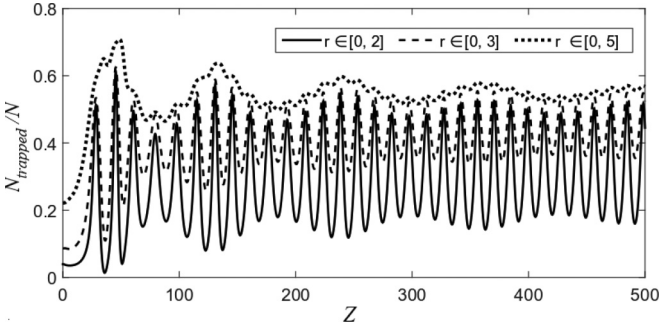
$$N_{trapped} = \int_0^{R_{trapped}} |A|^2 d\vec{r}.$$

FIG. 2. Evolution of the power trapped inside the small region around the hole. $R_{\text{trapped}} = 2$—solid line, $R_{\text{trapped}} = 3$—dashed line, $R_{\text{trapped}} = 5$—dotted line,

Different lines correspond to the radii of the observed regions. It is seen that in the central area with the radius of 2 the confined power is changing between approximately 20% and 50% of the total power, and for the area with the radius of 5, it is above 50% of the power of the initial Gaussian beam with $a = 10$.

This "nonlinear tapering" effect can potentially be useful in different applications. For instance, it can be used for a spatial transfer of light power from a broad area (defined by the high-power pumping sources) to a narrow core. Some classes of high-power fiber lasers exploit cladding pumping within a double-clad fiber structure. The first cladding has a substantially larger area (diameter $> 100\ \mu$m) compared with that the core, allowing the efficient launch of the output from the multimode pump sources with poor beam quality, such as, e.g., high-power laser diodes. The pump light is then partly propagates in the single-mode core where it is absorbed by the laser-active ions. The nonlinear lens potentially can provide a new design option for an efficient spatial compressor of the low-brightness high-power radiation of the laser diodes into a high brightness high-power laser beam coming out of the small active fiber core.

IV. SOLITON SOLUTIONS

Arrest of a wave collapse typically corresponds to the existence of stable solitons that provide a balance among diffraction and dispersion, and nonlinearity [17]. Therefore, next we examine localized steady-state solutions in the considered medium. Note that nonlinear waves in the layered structures in the one-dimensional case have been studied (see, e.g., Refs. [18,19]. In one-dimensional geometry an interplay between linear wave guiding and nonlinearity can lead to nonlinear surface waves. There are two major different features from that works in the problem we consider here. First, in the two-dimensional (2D) case nonlinear dynamics can lead to self-focusing and wave collapse, that is different from the one-dimensional systems considered in Refs. [18,19]. Second, as with what was mentioned before, there is no need for a linear wave guiding in the system we study.

It is well known that in the framework of the pure NLS equation, two-dimensional solitons, the so-called Townes modes [20] are unstable. In the considered here case of the 2D NLSE with a nonuniform distribution of nonlinearity, we
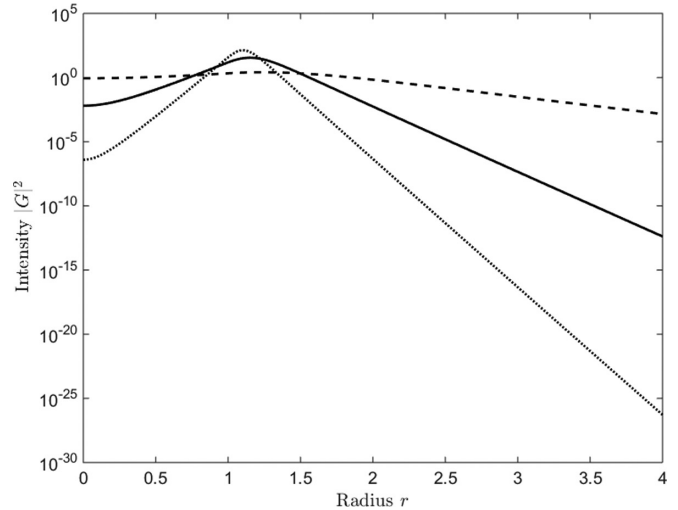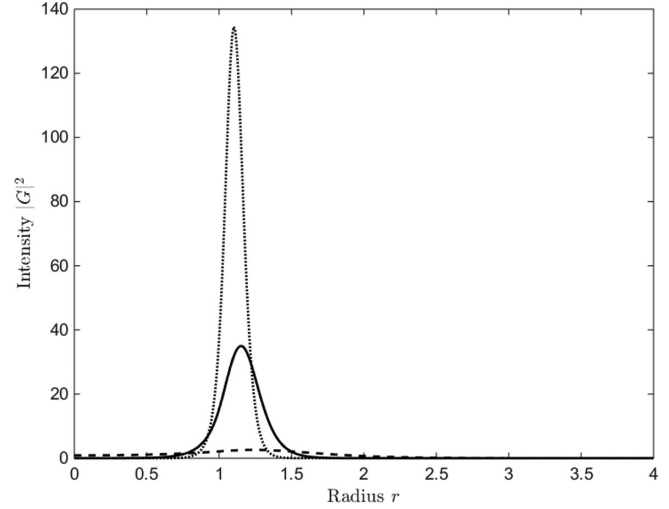

FIG. 3. Intensity distribution $|G(r)|^2$ for steady-state solutions in linear (top) and logarithmic (bottom) scales for different values of parameter λ ($\lambda = 1$—dashed line, $\lambda = 4$—solid line, and $\lambda = 8$—dotted line).

observe stable 2D soliton structures with a ring-type intensity distribution and similar breathing solutions. Their properties are illustrated in Figs. 3 and 4. Consider steady-state solutions of Eqs. (2) having the form of nonlinear localized solitary waves propagating in the z direction, $A(x, y, z) = \exp(i\lambda z)G(x, y)$. The waveform of such 2D solitons is described by the following equation [17]:

$$\frac{\delta}{\delta G^*}(H + \lambda N) = \lambda G - \frac{1}{2}\nabla_\perp^2 G - V(x, y)|G|^2 G = 0. \quad (3)$$

This means, in particular, that such solutions should correspond to stationary points of Hamiltonian H for a fixed power N. This equation can be seen as a stationary solution of some auxiliary relaxation process $M(G)G = 0$ with the *nonlinear* operator M given as

$$M(G) = \lambda - \frac{1}{2}\nabla_\perp^2 - V(x, y)|G|^2.$$

We have used a specific relaxation method in order to find stationary solutions described by e Eq .(3). A naive relaxation
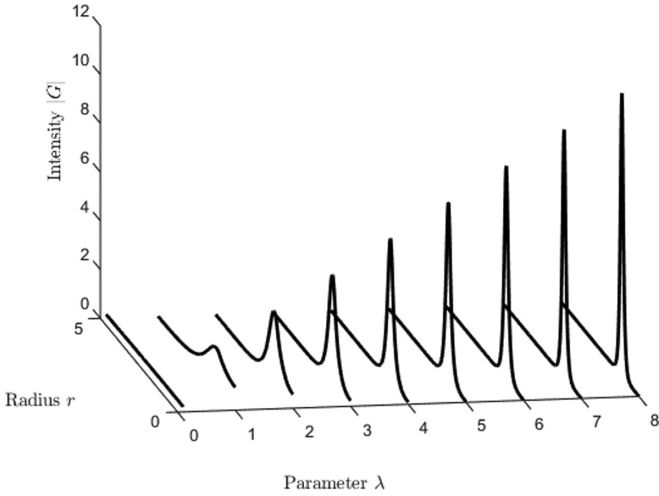
FIG. 4. Family of the soliton solutions for different parameters λ.

FIG. 5. Hamiltonian H of the soliton solutions of Eq. (3) versus power N.

method would utilize $\partial G/\partial \tau = M(G)G$, which would relax to a stationary solution $M(G)G = 0$ if it was stable which is rarely the case. In order to enforce convergence, we modify the relaxation problem to

$$\frac{\partial}{\partial \tau} M(G)G = -M(G)G. \qquad (4)$$

A formal solution of such a relaxation process would be schematically expressed as $M(G)G = M(G)G|_{\tau=0} e^{-\tau}$ which ultimately decays to zero to yield the target of $M(G)G = 0$.

One can arrange the iterative relaxation process by performing a differentiation in Eq. (4) in τ and introducing a new field variable $Q = \partial G/\partial \tau$,

$$\lambda Q + \tfrac{1}{2}\Delta Q + 3V(r)G^2 Q = \lambda G + \tfrac{1}{2}\Delta G + V(r)G^2 G.$$

Note that this equation is now *linear* in Q which allows to construct a recurrent iteration process,

$$\lambda Q_m + \tfrac{1}{2}\Delta Q_m + 3V(r)G_m^2 QQ_m = \lambda G_m + \tfrac{1}{2}\Delta G_m$$
$$+ V(r)G_m^2 G_m,$$
$$G_{m+1} = G_m + \Delta \tau Q_m.$$

A reduction to the algebraic iteration problem is achieved by approximation of Laplacian operator with a finite difference stencil, e.g., three point central difference stencil. Then the procedure is reduced to
  (1) start with a starting guess G_0;
  (2) find Q_0;
  (3) update G;
  (4) break and stop when the residue error is small enough;
  (5) repeat the cycle.
The resulting steady-state solutions are the functions of the coordinates (x, y) as well as parameters λ. Families of such multidimensional solutions are shown in Fig. 3.

Figure 3 illustrates intensity distribution in the steady-state ring solitons. Nonuniform distribution of nonlinearity creates the effective potential with power localized at the ring as opposite to the monotonic 2D solitons in the uniform NLSE-Townes modes. Figure 4 explicitly shows dependence of the ring soliton shape on the parameter λ.
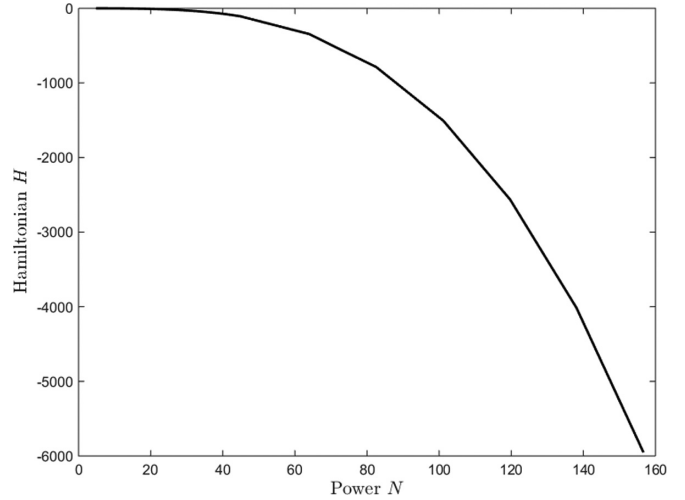
The observed solitons have sign-definite negative derivative dH/dN as illustrated in Fig. 5, that is a typical signature of the stable solitons in line with the Kolokolov-Vakhitov stability criterion [21].

V. VARIATIONAL APPROACH

Consider a standard variational [17] approach to demonstrate that a linear core leads to the appearance of a minimum in the Hamiltonian as opposite to the classical 2D NLS equation. Rewriting Eq. (2) in the Lagrangian form $\partial L/\partial A^* = 0$ with the Lagrangian L,

$$L = \pi \int_0^\infty r\,dr(iA^*A_z - AA_z^*) - H. \qquad (5)$$

Examples of the contraction dynamics and the soliton solutions presented above suggest the double scale ring shape beam profile, hence, the two parameter trial function is needed. Let us consider the trial profile as Gaussian with the width $a(z)$ multiplied by $\cosh[b(z)r/a(z)]$ so that for $b(z) > 1$ the beam maximum is off-center,

$$A(r) = \frac{\sqrt{N}\exp\left(-\frac{r^2}{2a^2}\right)\cosh\left(\frac{br}{a}\right)}{a\sqrt{J(b)\pi}}\exp(i\mu r^2/2 - i\nu r + ikz),$$
$$(6)$$

$$J(b) = 2\int_0^\infty x\,dx\,\exp(-x^2)\cosh^2(bx)$$

$$= 1 + b\exp(b^2)\int_0^b dt\,\exp(-t^2), \qquad (7)$$

where μ, ν, a, and b are functions of z.

We demonstrate below that is convenient to make a transform from the variables $(a; b)$ to mean radius $s = \bar{r}$ and mean square deviation $w = \sqrt{\bar{r^2} - \bar{r}^2}/a$ because the substitution of the exact solution $A(x, y, z)$ with a two-scale trial function in the form of Eq. (6) yields reduced equations on the parameters of the trial function in the form of Newton equations for the

motion in the two-dimensional potential $W(s, w)$,

$$\frac{d^2s}{dz^2} = -\frac{\partial W}{\partial s}, \qquad \frac{d^2w}{dz^2} = -\frac{\partial W}{\partial w}. \qquad (8)$$

Here $w = a\sqrt{3/2 + b^2 - C^2(b) - (1 + b^2)/[2J(b)]}$ and $s = aC(b)$, where $C(b) = \sqrt{\pi}\,[1 + (1 + b^2)\exp(b^2)]/[4J(b)]$. The potential $W(s, w)$ is obtained from $W(a, b)$ as introduced below in Eq. (13) by the transform $(a, b) \rightarrow (s, w)$.

Straightforward calculation of the mean values s and w leads to the explicit transform from the pair $(a; b)$ to $(s; w)$,

$$\frac{s}{a} = \frac{\bar{r}}{a} = \frac{1}{J(b)} \int_0^\infty x^2 dx \, \exp(-x^2)[1 + \cosh(2bx)]$$

$$= \frac{\sqrt{\pi}}{4J(b)}[1 + (b^2 + 1)e^{b^2}] = C(b), \qquad (9)$$

$$\frac{\bar{r^2}}{a^2} = \frac{1}{J(b)} \int_0^\infty x^3 dx \, \exp(-x^2)[1 + \cosh(2bx)]$$

$$= 3/2 + b^2 - \frac{1 + b^2}{2J(b)}, \qquad (10)$$

$$\frac{w}{a} = \sqrt{\frac{\bar{r^2} - (\bar{r})^2}{a^2}}$$

$$= \sqrt{3/2 + b^2 - \frac{1 + b^2}{2J(b)} - C^2(b)} = D(b). \qquad (11)$$

Finally, the substitution of the trial profile into the Lagrangian yields

$$L = \pi \int_0^\infty r\, dr(iA^*A_z - AA_z^*) - H$$

$$- k + \frac{d[\mu(\bar{r})^2]}{2\, dz} - \frac{d\mu}{dz}\sigma^2/2 + \frac{d(v - \mu\bar{r})}{dz}\bar{r}$$

$$- H(\mu, v; a, b),$$

$$H(\mu, v; a, b) = \pi \int_0^\infty r\, dr\left|\frac{dA}{d\bar{r}}\right|^2 - \pi \int_1^\infty r\, dr|A|^4$$

$$= N\frac{\mu^2\sigma^2 + (\mu\bar{r} - v)^2}{2} + NW(a, b), \qquad (12)$$

$$W(a, b) = W_1 - NW_2, \quad W_1 = \frac{1}{4a^2}\left(1 + \frac{1 - b^2}{J(b)}\right),$$

$$W_2 = \frac{1}{4a^2J^2(b)\pi}[\exp(-2/a^2)\cosh^4(b/a)$$

$$+ b\int_{1/a}^\infty dx \, \exp(-2x^2)[\sinh(2bx) + \sinh(4bx)/2].$$

$$(13)$$

Figures 6 and 7 illustrate the landscape of the potential W in variables (a, b) and (s, w) correspondingly. It is seen that both surfaces have the local minima corresponding to the stationary solutions (solitons).

This choice of the trial function reflects the two scale field distribution observed in the exact solution obtained numerically. Figure 8 shows comparison of the numerically found soliton solution with the trial function with the same value of power N.
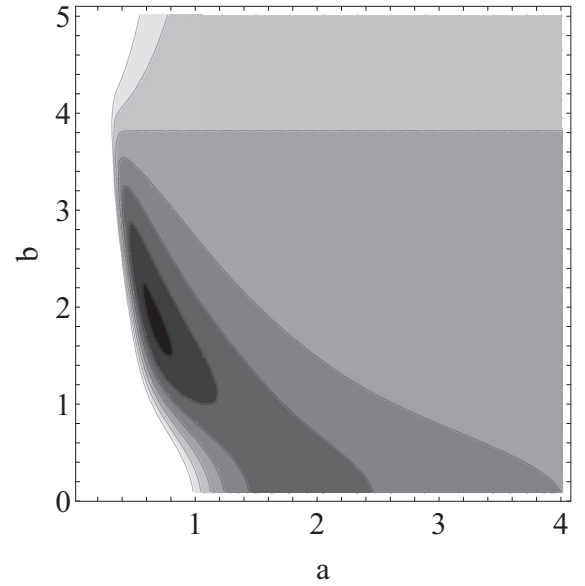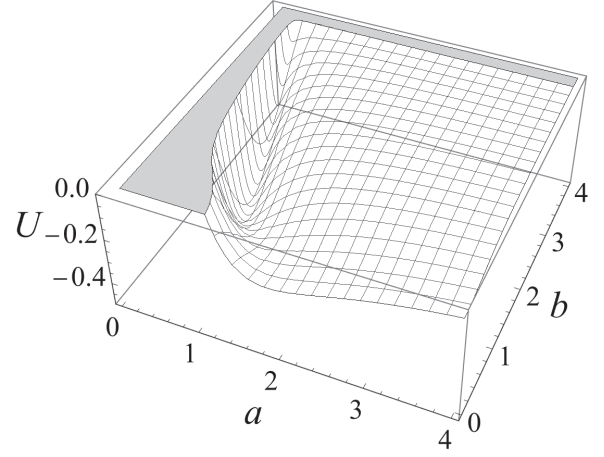

FIG. 6. Potential $W(a, b)$. Minimum at $a_s \approx 0.673\,256$ and $b_s \approx 1.839\,93$ corresponds to a stationary point (soliton).
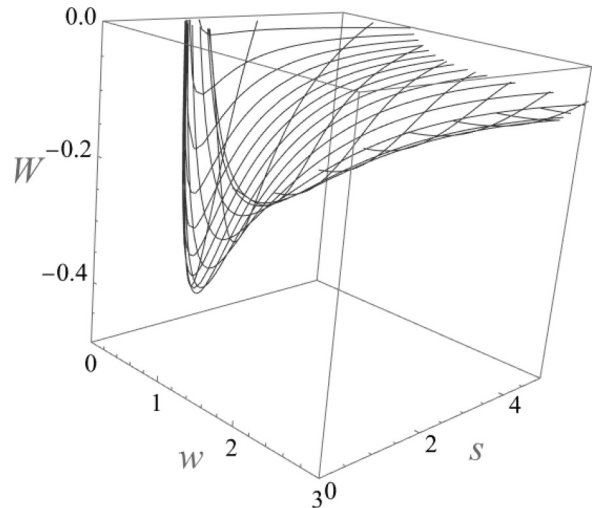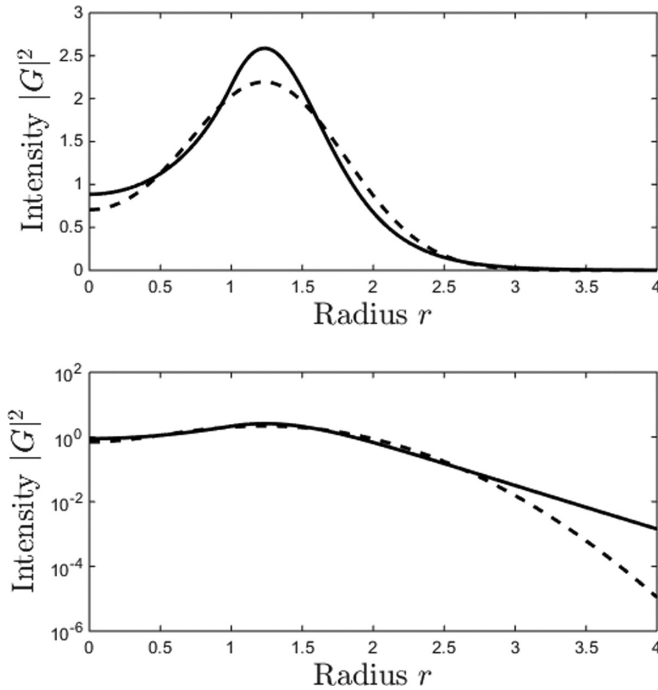

FIG. 7. Potential $W(s, w)$.

FIG. 8. Comparison of intensity profiles $|G(r)|^2$ for numerically found steady-state solutions and the corresponding trial function for $\lambda = 1$ in linear (top) and logarithmic (bottom) scales. Trial function corresponds to the stationary point of potential $U(a, b)$ with $a \approx 0.788\,213$ and $b = 1.5833$.

Evidently, Eq. (8) conserves a Hamiltonian H defined as $2H = (ds/dz)^2 + (dw/dz)^2 + 2WU(s, w) = $ const. The potential $U(s, w)$ has the minimum corresponding to the ring soliton.

VI. CONCLUSION

In general, formation of spatially localized states (solitons or breathers) from plane waves is of interest in various areas of science and practical applications [2,3,5,16,22–25]. Nonlinear instabilities and a wave collapse are examples of the energy localization mechanisms in nonlinear systems. For instance, a possibility of strong spatial localization of electromagnetic fields beyond the classical diffraction limit is related to the spatial resolution problem in optics. Controlled spatial (or temporal) localization of the the field at a certain distance (or at some moment in time) is important for energy transfer, laser processing of materials, and various other applications.

In conclusion, we proposed to use a medium with the nonuniform distribution of the nonlinear refraction parameter $n_2(x, y)$ in a way that the self-focusing of a broad initial distribution of the field (e.g., pumping wave) starts because the condition of self-focusing is satisfied in the outer region. However, the nonlinear beam narrowing is stopped by the dramatic decrease in n_2 in the central hole and core where power is focused. We demonstrate through numerical modeling that in contrast to the two-dimensional NLS equation, in the considered model, stable ring solitons can be formed.

[1] V. L. V. Zakharov and G. Falkovich, Kolmogorov spectra of turbulence i: Wave turbulence, Bull. Amer. Math. Soc. **29**, 304 (1993).

[2] R. W. Boyd, S. G. Lukishova, and Y. R. Shen, Eds. *Self-focusing: Past and Present. Fundamentals and Prospects*, edited by R. W. Boyd, S. G. Lukishova, and Y. R. Shen, (Springer, New York, 2009).

[3] C. Sulem and P. L. Sulem, *Nonlinear Schrödinger Equations: Self-Focusing and Wave Collapse* (World Scientific, New York, 1999).

[4] J. J. Rasmussen and K. Rypdal, Blow-up in nonlinear schroedinger equations-i a general review, Phys. Scr. **33**, 481 (1986).

[5] L. Bergé, Wave collapse in physics: Principles and applications to light and plasma waves, Phys. Rep. **303**, 259 (1998).

[6] Y. S. Kivshar and D. E. Pelinovsky, Self-focusing and transverse instabilities of solitary waves, Phys. Rep. **331**, 117 (2000).

[7] M. D. Feit and J. A. Fleck, Beam nonparaxiality, filament formation, and beam breakup in the self-focusing of optical beams, J. Opt. Soc. Am. B **5**, 633 (1988).

[8] G. Fibich and G. Papanicolaou, Self-focusing in the perturbed and unperturbed nonlinear schrodinger equation in critical dimension, SIAM J. Appl. Math. **60**, 183 (1999).

[9] S. Turitsyn, Spatial dispersion of nonlinearity and stability of multidimensional solitons, Theor. Math. Phys. **64**, 797 (1985).

[10] O. Bang, W. Krolikowski, J. Wyller, and J. J. Rasmussen, Collapse arrest and soliton stabilization in nonlocal nonlinear media, Phys. Rev. E **66**, 046619 (2002).

[11] J. Moloney and A. Newell, Nonlinear optics, Physica D **44**, 1 (1990).

[12] S. N. Vlasov, V. A. Petrishchev, and V. I. Talanov, Average description of wave beams in linear and nonlinear media, Izv. Vyssh. Uchebn. Zaved., Radiofiz. **14**, 1353 (1971).

[13] B. J. leMesurier, P. L. Christiansen, Y. B. Gaididei, and J. J. Rasmussen, Beam stabilization in the two-dimensional nonlinear schrödinger equation with an attractive potential by beam splitting and radiation, Phys. Rev. E **70**, 046614 (2004).

[14] O. A. Ladyzhenskaya, *The Mathematical Theory of Viscous Incompressible Flow* (Gordon and Breach, New York/London/Paris, 1969), Vol. XVIII, p. 224.

[15] S. K. Turitsyn, Nonstable solitons and sharp criteria for wave collapse, Phys. Rev. E **47**, R13 (1993).

[16] V. E. Zakharov and E. A. Kuznetsov, Solitons and collapses: Two evolution scenarios of nonlinear wave systems, Phys.-Usp. **55**, 535 (2012).

[17] E. Kuznetsov, A. Rubenchik, and V. Zakharov, Soliton stability in plasmas and hydrodynamics, Phys. Rep. **142**, 103 (1986).

[18] N. Akhmediev, Novel class of nonlinear surface waves: Asymmetric modes in a symmetric layered structure, Zh. Eksp. Teor. Fiz **83**, 545 (1982).

[19] P. J. Torres, Guided waves in a multi-layered optical structure, Nonlinearity **19**, 2103 (2006).

[20] R. Y. Chiao, E. Garmire, and C. H. Townes, Self-Trapping of Optical Beams, Phys. Rev. Lett. **13**, 479 (1964).

[21] N. G. Vakhitov and A. Kolokolov, Stationary solutions of the wave equation in a medium with nonlinearity saturation, Radiophys. Quantum Electron. **16**, 783 (1973).

[22] J. Marburger, Self-focusing: Theory, Prog. Quantum Electron. **4**, 35 (1975).

[23] E. Knobloch, Spatial localization in dissipative systems, Annu. Rev. Condens. Matter Phys. **6**, 325 (2015).

[24] P. M. Lushnikov and N. Vladimirova, Nonlinear combining of laser beams, Opt. Lett. **39**, 3429 (2014).

[25] M. Berry, N. Zheludev, Y. Aharonov, F. Colombo, I. Sabadini, D. C. Struppa, J. Tollaksen, E. T. F. Rogers, F. Qin, M. Hong, X. Luo, R. Remez, A. Arie, J. B. Götte, M. R. Dennis, A. M. H. Wong, G. V. Eleftheriades, Y. Eliezer, A. Bahabad *et al.*, Roadmap on superoscillations, J. Opt. **21**, 053002 (2019).